JMHT: Journal of Medicine and Health Technology
Vol. 01, No. 01, May, 2024, pp. 50-58
ISSN: 3046-6865
DOI: 10.12962/j30466865.v1i1.1214

Strength Assessment of Prosthetic Pylon Considering the Geometric of Raw Material

Achmad Syaifuddin[1], Dika Andini Suryandari[2], Helena Carolina Kis Agustin[3]
[1]Department of Medical Technology, Faculty of Medicine and Health, Institut Teknologi Sepuluh Nopember, Jl. Teknik Kimia, Keputih, Kec. Sukolilo, Surabaya, Jawa Timut, 60111, Indonesia
[2]Department of Mechanical Engineering Industry, Faculty of Vocation, Institut Teknologi Sepuluh Nopember, Jl. Teknik Kimia, Keputih, Kec. Sukolilo, Surabaya, Jawa Timut, 60111, Indonesia
[3]Department of Mechanical Engineering, Faculty of Industrial Technology and Engineering System, Institut Teknologi Sepuluh Nopember, Jl. Teknik Kimia, Keputih, Kec. Sukolilo, Surabaya, Jawa Timut, 60111, Indonesia

Corresponding Author: syaifudin@its.ac.id

Abstract — Prosthetic limbs are crucial as assistive devices for individuals with lower limb amputations. This study focuses on designing and analysing prosthetic feet, specifically the telescopic tube component, to achieve optimal material strength and aesthetic appeal. Numerical simulations using ANSYS Workbench 19 are conducted to assess the total deformation and von Mises stress. Design iterations adjust the pylon tube thickness and material selection. Prototypes are developed using aluminium 6061 tube and rod materials for further testing. Various tests, including scanning electron microscopy, metallography, axial tensile testing, and tangential tensile testing (according to ASTM B 557M), are performed to evaluate the material properties. Results indicated that the axial and yield strengths of the aluminium 6061 rod are superior to the tube type. Conversely, the aluminium 6061 tube exhibits higher ultimate and yield stability in tangential testing. Ultimately, the study concludes that the aluminium 6061 tube material is more robust and suitable for prosthetic feet.

Keywords — Prosthetic limb; telescopic pylon; numerical analysis; material strength; aesthetic appeal; aluminium 6061.

How to cite: Syaifuddin A, Suryandari D A, Agustin C K. Strength Assessment of Prosthetic Pylon Considering the Geometric of Raw Material. Journal of Medicine and Health Technology. 2024.

Manuscript received 14 May 2024; revised 18 May 2024; accepted 20 May 2024. Date of publication 30 May 2024.
JMHT is licensed under a Creative Commons Attribution-Share Alike 4.0 International License.

INTRODUCTION

Prosthetic limbs are pivotal in improving the mobility and quality of life of individuals with lower limb amputations. Among the critical components of prosthetic feet, the design and analysis of the telescopic tube component hold significant importance due to their influence on material strength and aesthetic appeal. This study aims to investigate the optimization of prosthetic feet design by focusing on the telescopic tube component, to achieve superior functionality.

Prosthetic feet can be designed and optimized using various methods. Namely, lower leg trajectory error (LLTE) optimization, a design objective for passive prosthetic feet that model the trajectory of the lower leg segment throughout a step for a given prosthetic foot and selects design variables to minimize the error between this trajectory and target physiological power [1], [2]. Also, energy-storing-and-releasing (ESR) prosthetic feet that store elastic energy in composite materials must be developed and optimized for stiffness, considering the loads a healthy human foot undergoes and its kinematics while walking [3].

Telescopic tubes are used in various applications, including prosthetic feet. The outer tube is typically made of lightweight and durable material, such as aluminium or carbon fibre, and provides the structure and support for the prosthetic foot. The inner tube is usually made of similar material and can slide within the outer tube to adjust the length of the foot. The locking mechanism secures the inner tube and prevents it from sliding out of the outer tube during use. The components of telescopic tubes used in prosthetic feet are designed to provide a lightweight, durable, and adjustable structure that can support the user's weight and provide a natural gait [4].

In the subsequent sections of this paper, we will delve into the methodology employed for the design and analysis of prosthetic feet, discuss the numerical simulations and experimental tests in detail, and present a comprehensive analysis of the material properties. By examining the potential benefits and limitations of the aluminium 6061 tube and rod materials, this research aims to inform the selection process and guide future advancements in prosthetic foot design.

Comprehensive testing was performed on the prototypes to evaluate the material properties. Various tests, including scanning electron microscopy, metallography, axial tensile testing, and tangential tensile testing, were conducted per ASTM B 557M standards. These tests aimed to assess the mechanical behaviour and characteristics of the materials under different loading conditions. By exploring material properties and testing methodologies, this study contributes to understanding the performance and suitability of different materials for prosthetic feet design. The findings from this research will aid in developing more robust and effective prosthetic limb solutions, ultimately improving the mobility and comfort of individuals with lower limb amputations.

MATERIALS AND METHOD

The mechanical performance of prosthetic feet was evaluated, allowing a comprehensive assessment of parameters such as total deformation and von Mises stress, providing valuable insights into the overall structural behaviour of the prosthetic feet. To enhance the performance, design iterations were conducted, incorporating adjustments to the pylon tube thickness and material selection. The selection process involved identifying materials that offer optimal properties for the prosthetic application. In this study, prototypes were developed using aluminium 6061 tube and rod materials. They were chosen for their favourable characteristics and suitability in prosthetic design.

Finite element analysis (FEA) is a widely used technique in mechanical simulation. It involves dividing a complex mechanical system or structure into smaller, simpler parts called finite elements and then analysing the behaviour of each under different conditions. FEA is used to predict the kinematics and contact of the patellofemoral joint through co-simulation of rigid body dynamics and nonlinear FEA [5]. In another research, FEA is used to simulate the mechanical stimuli of trabecular bone in osteoporosis. The distribution of Von Mises stress, octahedral strain, strain energy density, fluid velocity, and pore pressure are predicted for the bone's solid and marrow phases [6]. FEA is also used to improvise the effective foot length ratio (EFLR) and progression of the centre of pressure (CoP) of a solid ankle-cushioned heel (SACH) in prosthetic feet [7], [8].

1. *Static Structure Analysis*

   Static structural analysis with finite element method simulations was conducted on two designs of prosthetic legs, namely transtibial and transfemoral. Both designs encompassed various ankle and knee joint variations. Figure 1 (a) illustrates a transtibial prosthetic leg with fixed ankle and single-axis types, which Figure 1 (b) showcases a transfemoral prosthetic leg with different ankle and knee joint variations.

(a) (b)

Fig. 1. Transtibial and transfemoral prosthetic leg

Both types of prosthetic legs, transtibial and transfemoral, will be further developed with telescopic features. The telescopic feature allows users to adjust the length of the prosthetic leg. This is necessary because the prosthetic leg used by individuals often undergoes changes in size over time due to usage. Therefore, this feature is suitable for users without repeated fittings.

Fig. 2. Telescopic prosthetic legs

The prosthetic leg with telescopic features is subjected to maximum level P8 conditions and loading, following ISO 10328 as a standard of prosthetic, with a weight limit of less than 175 kg. Two boundary conditions are applied.

The total deformation and von Mises equivalent stress of the prosthetic leg is obtained in the research simulation. This data serves as a reference for material recommendations. Total deformation is represented in deflection data that occurs during loading. At the same time, von Mises stress predicts material failure if the von Mises stress reaches the material's yield strength, Sy.

The simulation results are then validated using simple manual calculations as an approximation approach. The stress calculations for conditions 1 and 2 are respectively $\sigma = 2.165\times 10^{-6}$ MPa and $\sigma = 1.092\times 10^{-6}$ MPa. These values are compared with the simulation results for conditions 1 and 2, which are 2.353×10^{-6} MPa and 1.455×10^{-6} MPa , respectively, indicating agreement. Thus, the multiplicative factors for conditions 1 and 2 are determined to be 0.92 and 0.75, respectively. Both materials prove to be suitable for application in prosthetic legs. However, considering the availability of raw materials in Indonesia, aluminium 6061 is the most adequate compared to aluminium 7075. Further research on aluminium 6061 is therefore warranted.

2. *Material Testing*

Comprehensive material testing is essential in validating the suitability and performance of materials in prosthetic limb applications. Testing should include mechanical properties such as tensile and bending tests, socket failure characteristics, and fatigue tests. The use of a robotic test rig, a mock residual limb, and mechanical testing protocol, and comparing kinetic and kinematic data from human subjects can also help evaluate the performance of prosthetic and robotic joints and improve prosthetic mobility[9]–[13].

The tested pylon tube used in several material tests is made of aluminium 6061. These tests aim to investigate the manufacturing process's influence on the prosthetic leg made from available raw materials. Aluminium 6061 is commonly known in both rod and tube forms, and it is found that they exhibit differences when manufactured into prosthetic legs. Therefore, several tests will be conducted on pylon tubes made from aluminium 6061 tubes and rods.

3. *Elemental Analysis Test*

The elemental analysis test was conducted using a Hitachi Flex SEM 1000 scanning electron microscope coupled with an Ametek Edax Apex series energy dispersive spectroscopy system. The results of elemental analysis are shown in Table 1 and Table 2.

Table 1. EDS test results of an aluminium 6061 rod compared to standard

No.	Material	Standard	Tests	Status
1.	Mg (%)	0.8-1.2	2.28	Exceed
2.	Al (%)	95.8-98.6	96.63	Appropriate
3.	Si (%)	0.4-0.8	0.40	Appropriate
4.	Cr (%)	0.04-0.35	0.26	Appropriate
5.	Cu (%)	0.15-0.4	0.44	Exceed

Table 2. EDS test results of an aluminium 6061 tube compared to standard

No.	Material	Standard	Tests	Status
1.	Mg (%)	0.8-1.2	1.73	Exceed
2.	Al (%)	95.8-98.6	97.39	Appropriate
3.	Si (%)	0.4-0.8	0.47	Appropriate
4.	Cr (%)	0.04-0.35	0.17	Appropriate
5.	Cu (%)	0.15-0.4	0.24	Appropriate

It is observed that the tested aluminium 6061 rod and tube are primarily composed of aluminium (Al), followed by magnesium (Mg). In the 6-series aluminium alloys, the primary alloying elements are magnesium and silicon, with magnesium being the predominant alloying element.

4. *Element Analysis Test*

The metallography testing was conducted by cutting the specimen's end and embedding it in resin, as shown in Figures 3 (a) and (b). The specimen was then wet ground using water and grit sizes of 80, 120, 300, 400, 600, 800, 1000, 1200, 1500, 2000, and 5000. Subsequently, the specimen was polished using a cloth pad with alumina powder and wiped with alcohol to remove any residue. The specimen was then etched using an etching solution composed of HCl (30 mL), HF (2.5 mL), HNO3 (40 mL), CrO3 (4.45 mL), and H2O (42.5 mL) for a duration of 60 seconds. After etching, the specimen was rinsed with alcohol once again, and the process of micrography could be carried out. The process could be repeated if the material structure was not yet visible.

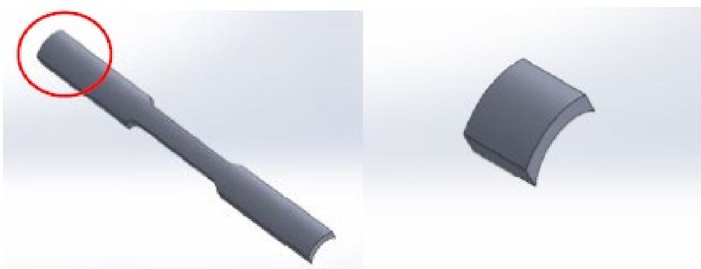

Fig. 3. Specimen cutting for metallography test

Testing was conducted for two specimens with each rod and tube material to obtain the best accuracy. The results of 100 times magnification microscopic photography of the aluminium 6061 for rod specimen are illustrated in Figures 4 (a) and (b), while for the tube specimen in Figures 5 (a) and (b).

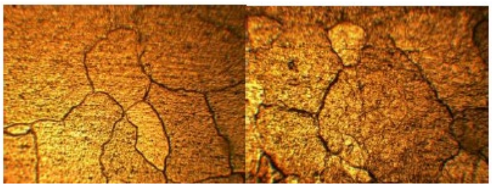

(a) (b)

Fig. 4. 100x magnification microscopic photography results of rod-type aluminum 6061 specimen

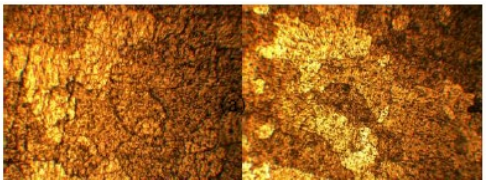

(a) (b)

Fig. 5. 100x magnification microscopic photography results of tube-type aluminum 6061 specimen

Figure 4 and Figure 5 above show that there are no significant differences between the tube-type and rod-type aluminum 6061 specimens.

5. *Metallography Test*

The axial tensile testing conducted in this research is based on the ASTM B 557M-02a, 2003 standard. The standard encompasses various testing methods and specimen types. For this study, the tensile testing method and specimen type employed are specific to tubular specimens. Within the tubular specimen category, two testing methods are available, namely thin-walled tubes and thick-walled tubes. This research focuses on thin-walled tubes, specifically those with a thickness value of 4 mm. The dimensional specifications for the tensile testing specimen in the form of a tube, following the ASTM B 557M.

The graph grabber application was utilized to digitize the tensile testing graphs, obtaining either graphical or coordinate data. The obtained coordinates were then scaled using the maximum force and elongation data. Subsequently, force-displacement graphs were generated for each specimen, as depicted in Figures 6 (a) to (e).

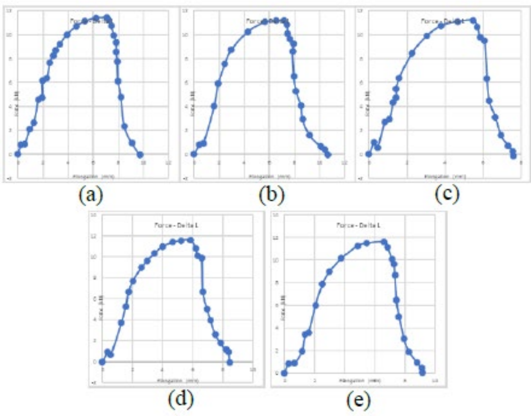

Fig. 6. Force-displacement graphs

The next step involves converting the force-displacement graphs into stress-strain graphs. The stress values are obtained using the equation:

$$\sigma_u = \frac{F_u}{A_0} \qquad \text{Eq. (1)}$$

Next, the force-displacement data is scaled to generate stress-strain graphs for specimens 1 to 5, which are shown in Figures 7 (a) to (e). This allows for the analysis of material properties such as yield strength, ultimate tensile strength, and strain-hardening behaviour.

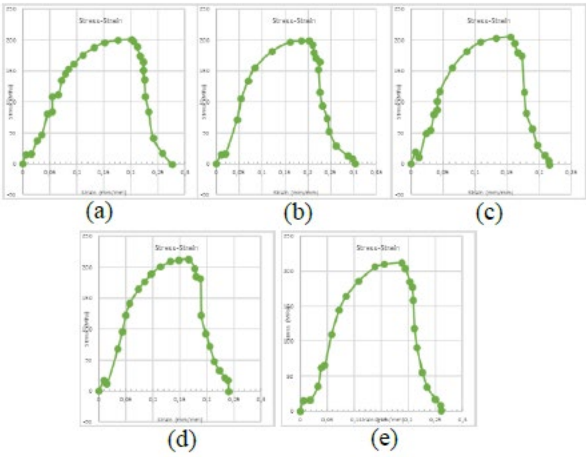

Fig. 8. Stress-strain graphs

After analysing the five stress-strain graphs, the yield points are determined using the 0.2% offset method. The offset line is created by drawing a straight line parallel to the elastic region of the graph and shifting it by 0.002 mm/mm. The yield values for each chart are determined using the graph grabber application. The obtained data is tabulated and averaged to obtain the final material properties of aluminium 6061 manufactured as rods. The resulting data is presented in Table 3.

Table 3. Material properties of rod-type aluminium 6061

Al6061 Axial Properties		
Specimen	Yield Strength (Mpa)	Tensile Strength (Mpa)
1.	144.9503	200.0702
2.	161.1918	198.476
3.	124.9481	204.978
4.	169.0349	213.1961
5.	151.8245	210.183

6. *Axial Tensile Testing*

Unlike conventional tensile tests that apply axial tensile loading along the specimen axis, the Ring Hoop Tensile Test (RHTT) is specifically designed to assess the resistance of pipe thickness. The RHTT consists of three main components: fixtures, D-blocks, pin, and the specimen, as illustrated in Figure 9. It is worth noting that the D-blocks exhibit three times the strength of the tested specimen.

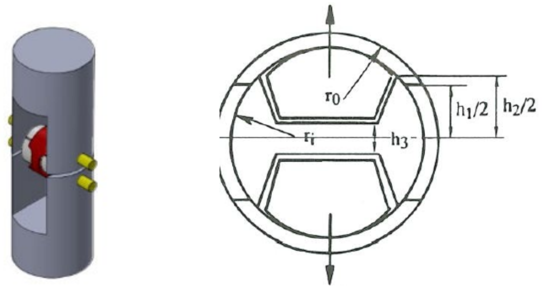

Fig. 9. Tangential tensile testing scheme

The tangential tensile testing employed in this research is based on previous studies conducted in various journals. These studies encompass different testing methods and specimen types. For this research, the testing involves the use of the ring hoop tensile test method with "dogbone" shaped D-Blocks, as depicted in Figure 10. In this type of tangential tensile testing, there is a gauge section or constriction area on both sides of the specimen, which is then positioned adjacent to the D-Block (on the right and left sides). This approach aims to minimize the occurrence of frictional forces that could compromise the purity of the tensile force measurements.

DISCUSSION

The simulation was conducted on both prosthetic feet using ISO 10328 standard: Prosthetics - Structural testing of lower-limb prostheses - requirements and test methods, precisely the highest level P7 load of 175 kg body weight, to obtain total deformation and von Mises stress. The allowable von Mises stress should be 75% of the yield strength of aluminium 6061, which is 207 MPa, while for aluminium 7075, it is 377.25 MPa. Design adjustments are required for the pylon tube to achieve a safe prosthetic foot, which involves increasing the thickness of the pylon tube to 4 mm, thus affecting the von Mises stress. From the simulation, it is found that both aluminium 7075 and 6061 are safe materials for prosthetic feet.

From the simulation, Von Mises stress for the transtibial pylon tube and for the transfemoral pylon tube are obtained. After evaluating the design by increasing the thickness of the pylon tube, the maximum von Mises stress is achieved. Both aluminium 7075 and 6061 can be used as materials for the pylon tube. However, considering the limited availability of suitable raw materials in Indonesia, aluminium 6061 is chosen. Further analysis and experiments on aluminium 6061 are needed.

The available raw material for aluminium 6061 consists of tubes and rods with different property ratios, as shown in Table 3 for both axial and tangential testing. The rod specimens exhibit higher axial strength than the tube specimens, while the tube specimens are more robust in terms of tangential strength. According to ASTM B 557M-02a, section XI.4.3, the difference in a cross-sectional area does not affect the ultimate material strength, considering the variations in thickness that occur during the design and manufacturing processes.

The tube specimens of aluminium 6061 are rod-shaped specimens processed further with heat treatment during production. As a result, the tube specimens have higher maximum and minimum strength compared to the rod-shaped models. In the tangential testing, the tube specimens exhibit higher strength than the tangential tensile strength of the rod-shaped specimens, and there is no significant strain hardening that causes a drastic increase in the strength of the aluminium tube.

CONCLUSION

From the numerical analysis conducted, the total deformation of the transfemoral prosthetic foot for aluminium 7075 and 6061 is 0.029365 m and 0.029854 m, respectively. For the transtibial type, the total deformations are 0.017421 m and 0.018129 m, respectively. The maximum von Mises equivalent stress obtained from the transfemoral and transtibial prosthetic feet results in maximum stresses that are deemed unsafe. This is indicated by the percentage of the maximum von Mises stress compared to the material's yield stress, which exceeds 75% for both aluminium 6061 and 7075.

Design adjustments by increasing the thickness of the pylon tube can affect the weight of the prosthetic foot and the maximum weight capacity of the user. In the case of aluminium 6061, when an additional thickness of 2 mm is added, it can achieve level P8 or accommodate a maximum user weight of 175 kg. The testing of aluminium 6061 rod and tube materials reveals that the aluminium 6061 tube exhibits higher strength compared to the rod type. This is evident from the ultimate strength and yield strength values, where the tube type yields 205.3807 MPa and 150.3899 MPa for axial loading, while for tangential loading, the values are 574.944 MPa and 561.9398 MPa, respectively.

ACKNOWLEDGEMENT

This work was supported by research grant funds from Institut Teknologi Sepuluh Nopember (ITS), prototype research [869/PKS/ITS/2020] and partnership research [1303/PKS/ITS/2021]. All authors acknowledge these supports.

REFERENCES

[1] Prost V, Olesnavage K, Winter A. Design And Testing Of A Prosthetic Foot Prototype With Interchangeable Custom Rotational Springs To Adjust Ankle Stiffness For Evaluating Lower Leg Trajectory Error, An Optimization Metric For Prosthetic Feet. Proceedings of the ASME Design Engineering Technical Conference. 2017. Available: http://www.asme.org/about-asme/terms-of-use

[2] Olesnavage K, Winter A. Design and preliminary testing of a prototype for evaluating lower leg trajectory error as an optimization metric for prosthetic feet. Proceedings of the ASME Design Engineering Technical Conference (American Society of Mechanical Engineers (ASME)). 2016. doi: 10.1115/DETC2016-60565.

[3] Tabucol J, Brugo T, Povolo M, Leopaldi M, Oddsson M, Carloni R, Zucchelli A. Structural fea-based design and functionality verification methodology of energy-storing-and-releasing prosthetic feet. Applied Sciences. 2022;12(1). doi: 10.3390/app12010097.

[4] Gabbiadini S, Bariani P, Savio E, Rizzi C. Knowledge-based design of lower limb prosthesis. Universita Degli Studi di Padova. 2011

[5] Müller J, Razu S, Erdemir A, Guess T. Prediction of patellofemoral joint kinematics and contact through co-simulation of rigid body dynamics and nonlinear finite element analysis. Comput Methods Biomech Biomed Engin. 2020;23(11):718–733. doi: 10.1080/10255842.2020.1761960.

[6] Sandino D, McErlain D, Schipilow J, Boyd S. Mechanical stimuli of trabecular bone in osteoporosis: A numerical simulation by finite element analysis of microarchitecture. J Mech Behav Biomed Mater. 2017;66:19–27. doi: 10.1016/j.jmbbm.2016.10.005.

[7] Balaramakrishnan T, Natarajan S, Srinivasan S. Roll-over shape of a prosthetic foot: a finite element evaluation and experimental validation. Med Biol Eng Comput. 2020;58(10):2259–2270. doi: 10.1007/s11517-020-02214-9.

[8] Balaramakrishnan T, Natarajan S, Sujatha S. Design of a Biomimetic SACH Foot: An Experimentally Verified Finite Element Approach. Journal of Biomimetics, Biomaterials and Biomedical Engineering. 2020;45:22–30. doi: 10.4028/www.scientific.net/JBBBE.45.22.

[9] Quinlan J, Yohay J, Subramanian V, Poziembo B, Fatone S. Using mechanical testing to assess the effect of lower-limb prosthetic socket texturing on longitudinal suspension. PLoS One. 2020;15(8):e0237841. doi: 10.1371/journal.pone.0237841.

[10] Sallal H, Kadhim A. Comparing the Mechanical Behavior of Lamination Resin Reinforced with Two Types of Organic and Inorganic Particles Used in Prosthetic Applications. Key Eng Mater. 2022;937:89–98. doi: 10.4028/p-9d9855.

[11] Jweeg M, Hammoudi Z, Alwan B. Optimised Analysis, Design, and Fabrication of Trans-Tibial Prosthetic Sockets. IOP Conf Ser Mater Sci Eng. 2018;433:012058. doi: 10.1088/1757-899X/433/1/012058.

[12] Etoundi A, Dobner A, Agrawal S, Semasinghe C, Georgilas I, Jafari A. A Robotic Test Rig for Performance Assessment of Prosthetic Joints. Front Robot AI. 2022;8. doi: 10.3389/frobt.2021.613579.

[13] Bekrater-Bodmann R, Kehl I, Hafner B, Ranker A, Giordano A, Franchignoni F. Rasch validation of the German translation of the Prosthetic Limb Users Survey of Mobility short forms in people with lower limb amputation. Prosthet Orthot Int. 2023;47(5):552-557. doi: 10.1097/PXR.0000000000000201.

[14] Hamzaid N, Yusof N, Jasni F. Sensory Systems in Micro-Processor Controlled Prosthetic Leg: A Review. IEEE Sens J. 2020;20(9):4544–4554. doi: 10.1109/JSEN.2019.2944653.

[15] Gao H, Luo J, Pi M, Li Z, Li Q, Zhao K, et.al. EEG-Based Volitional Control of Prosthetic Legs for Walking in Different Terrains. IEEE Transactions on Automation Science and Engineering. 2021;18(2):530–540. doi: 10.1109/TASE.2019.2956110.

[16] Rizqillah R. Material Selection of Below-knee Leg Prosthetics. Journal of Materials Exploration and Findings. 2022;1(1). doi: 10.7454/jmef.v1i1.1004.

[17] Debta S, Kumar K. Static Structural Analysis of a Powered Ankle Foot Prosthesis Mechanism. 2018;5(5). Available: https://www.sciencedirect.com/science/article/abs/pii/S2214785318303341

[18] Embry K, Gregg R. Analysis of Continuously Varying Kinematics for Prosthetic Leg Control Applications. IEEE Transactions on Neural Systems and Rehabilitation Engineering. 2021;29:262–272. doi: 10.1109/TNSRE.2020.3045003.

[19] Quintero D, Martin A, Gregg R. Toward Unified Control of a Powered Prosthetic Leg: A Simulation Study. IEEE Transactions on Control Systems Technology. 2018;26(1):305–312. doi: 10.1109/TCST.2016.2643566.

[20] Shastry G, Toby A, Kumbhar M, Salunkhe V, Jagadeesha T. Simulation and optimization of materials used for prosthetic leg for above-knee amputees using MR fluid. Elsevier Ltd. 2021;45:5292–5298. doi: 10.1016/j.matpr.2021.01.862.

[21] Kadhim F, Chiad J, Takhakh A. Design and Manufacturing Knee Joint for Smart Transfemoral Prosthetic. IOP Conference Series: Materials Science and Engineering. 2018. doi: 10.1088/1757-899X/454/1/012078.

[22] Beck O, Taboga P, Grabowski A. Sprinting with prosthetic versus biological legs: Insight from experimental data. R Soc Open Sci. 2022;9(1). doi: 10.1098/rsos.211799.

[23] Chakravarthy Y, Vigneshwar P, Kedarnath P, Saiharish Y, Srinath A. Optimum Material Selection to Prosthetic Leg through Intelligent Interface of RSM and FEA. 2017;4(2):1998-2007. doi:10.1016/j.matpr.2017.02.046

[24] Oleiwi J, Hadi A. Properties of Materials and Models of Prosthetic Feet: A Review. IOP Conf Ser Mater Sci Eng. 2021;1094(1):012151. doi: 10.1088/1757-899x/1094/1/012151.

[25] EL-Bagory T, Younan M, Alarifi, I. Failure Analysis of Ring Hoop Tension Test (RHTT) Specimen under Different Loading Conditions. Proceedings of the ASME Design Engineering Technical Conference (American Society of Mechanical Engineers (ASME)). 2018. https://doi.org/10.1115/PVP2018-84198

[26] Kuswanto D, Dhafin F, Syaifudin A, Rahman M. Customizable Design of 3D Printed Body Powered Prosthesis for Trans-Radial and Shoulder Disarticulation Amputees. 2019 2nd International Conference on Bioinformatics, Biotechnology and Biomedical Engineering (BioMIC) - Bioinformatics and Biomedical Engineering. 2019. doi: 10.1109/BioMIC48413.2019.9034701.

[27] Király M, Antók D, Horváth L, Hózer Z. Evaluation of axial and tangential ultimate tensile strength of zirconium cladding tubes. Nuclear Engineering and Technology. 2018;50(3):425–431. doi: 10.1016/j.net.2018.01.002.

[28] Rachmat N. Penggunaan Kaki Palsu Terhadap Kepercayaan Diri Pasien Post Amputasi Kaki. Jurnal Kesehatan. 2016

[29] Junianto A, Kuswanto D. Desain Kaki Palsu untuk Membantu Aktivitas Berjalan pada Tuna Daksa Transtibial dengan Menggunakan Rapid Prototyping dan Reverse Engineering. Jurnal Sains dan Seni ITS. 2018;7(1). doi: 10.12962/j23373520.v7i1.29934.

[30] Hidayat M, Eryk I, Ronilaya F, Alfarizi M. Design and Analysis of Remote Load Measurement and Control System on a Hybrid Power Plant Prototype. Proceedings - IEIT 2021: 1st International Conference on Electrical and Information Technology. 2021. doi: 10.1109/IEIT53149.2021.9587417.